AIAA JOURNAL
Vol. 30, No. 5, May 1992

Similarity in Supersonic Mixing Layers

Otto Zeman*
Stanford University, Stanford, California 94305

This paper deals with similarity and parameterization in supersonic shear layers with isothermal freestreams, when the Mach number M (based on the velocity difference ΔU across the layer) is $M \geq 3$. With the support of modeling results and experiments, it is argued that under these conditions the turbulent velocity fluctuations are controlled by the local sonic speed, and the rms fluctuating Mach number M_t approaches a saturation limit. These conditions permit inference of similarity laws and parametric expressions for the shear layer growth, maximum centerline magnitudes of temperature (or density), and Reynolds stresses. Turbulence closure simulations are shown to corroborate the proposed similarity theory and parameterization. An extension of the theory for mixing layers with different densities in the freestreams is also proposed.

Nomenclature

a	= sonic speed
C_δ	= normalized growth rate defined in Eq. (18)
c_p	= specific heat
F	= dilatation function defined in Eq. (11)
f	= velocity similarity function defined in Eq. (12)
f_p	= function defined in Eq. (10)
H, h	= enthalpy
K, K_h	= eddy viscosity and conductivity
ℓ	= turbulence length scale
M	= shear layer Mach number, $\Delta U/a_o$
M_t, M_c	= rms (turbulent) and convective Mach numbers
P, p	= static pressure
P_{rt}	= turbulent Prandtl number, K/K_h
q^2	= twice turbulent kinetic energy, $\widetilde{u_i u_i}$
R_e	= turbulent Reynolds number
R_T	= shear layer Reynolds number defined in Eq. (18)
S	= similarity function defined in Eq. (24)
T	= static temperature
U_i	= total velocity component
u'	= turbulence velocity scale, $\sqrt{q^2/3}$
u_i	= fluctuating velocity component ($u_1 = u$, $u_2 = v$, $u_3 = w$)
$x = x_1, y = x_2$	= streamwise and transverse coordinates
α, β	= constants
γ	= specific heat ratio
δ_ω	= vorticity thickness of a shear layer
ε_s	= solenoidal dissipation
ε_d	= dilatational dissipation $\approx \nu\overline{(u_{j,j})^2}$
η	= transverse similarity variable
θ	= temperature similarity function defined in Eq. (13)
κ	= molecular conductivity
μ, ν	= dynamic and kinematic viscosities
ρ, ρ'	= density, density fluctuations
ψ	= streamfunction

Subscripts

c	= layer centerline location
o	= freestream condition
1, 2	= designating fast and slow freestream

Superscripts

$\sim$	= Favre average
$-$	= Reynolds or ensemble average
$'$	= derivative with respect to x or η

I. Introduction

THE most prominent, observed effect of compressibility on mixing layers is inhibition of the layer growth (Bogdanoff,[1] Papamoschou and Roshko,[2] Ikawa and Kubota,[3] Chinzei et al.,[4] Samimy and Elliot,[5] and others). The findings have been unified by the concept of the so-called convective Mach number (M_{co}) introduced by Bogdanoff,[1] and Papamoschou and Roshko,[2] wherein properly normalized growth rates are expected to be solely a function of M_{co}. The experimental data suggest that the growth rate decreases appreciably for convective Mach numbers between 0.3 and 1.2; beyond $M_{co} = 1.5$ the growth rates level off at about 30% of the low speed value. Zeman[6] suggested that growth inhibition in mixing layers is a consequence of additional (anamalous) dissipation due to the presence of fluctuating dilatation $u_{j,j}$. This so-called dilatation dissipation ε_d occurs in regions where fluid elements acquire supersonic relative speeds and form shock-like structures, or turbulent shocklets. Recently, the turbulent shocklets have been identified both in decaying (Lee et al.[7]), and shear-driven turbulence (Blaisdell et al.[8]). The dilatation dissipation ε_d augments the solenoidal (Kolmogorov) dissipation ε_s, and so reduces turbulence intensities and mixing layer growth; ε_d has been found to be expressible in the form $\varepsilon_d/\varepsilon_s = F(M_t)$. In mixing layers, ε_d is expected to become important when the Mach number M (based on the relative velocity difference $\Delta U = U_1 - U_2$ of the freestreams) is about one. This corresponds to $M_{co} \approx 1/2$, the onset of growth rate reduction.[1-5]

There exists so far no definite physical explanation for the observed leveling of growth rates at convective Mach numbers $M_{co} > 1.2$. Fig. 1 shows that the Zeman model[6] which includes the dilatation dissipation effect is in qualitative agreement with experimental data and predicts the growth rate leveling for $M_{co} \geq 1.5$. It is, therefore, plausible that for larger Mach numbers, the dilatation dissipation affects the turbulence so that the turbulent fluctuations (and also the layer growth rate) are determined by the local sonic velocity rather than by the velocity difference ΔU. Evidence for this is shown in Fig. 2 (also Fig. 5 in Ref. 6) where the modeled maxima of the rms

Received Jan. 28, 1991; revision received Aug. 12, 1991; accepted for publication Aug. 19, 1991.

*Senior Research Fellow, Center for Turbulence Research.

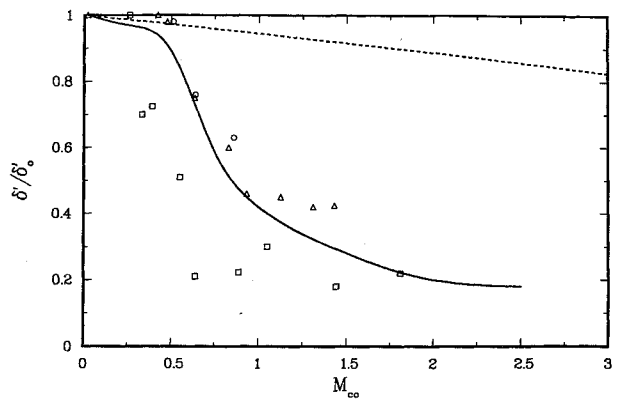

Fig. 1 Normalized shear layer growth rates vs convective Mach number M_{co}. The solid line represents the model simulations based on the Pitot probe thickness (δ_p); dashed line is the simulations without the dilatation dissipation; experimental data points labeled (□) are from Ref. 2; (△) from Ref. 1; and (○) from Ref. 5.

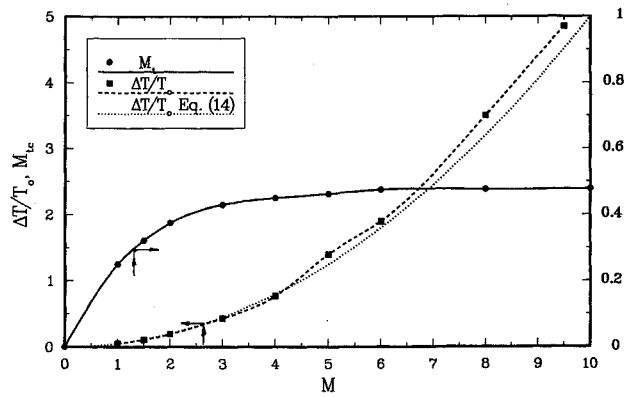

Fig. 2 Model-computed rms Mach number M_t and the centerline temperature excess $\Delta T/T_o$ as functions of the Mach number M.

Mach number M_t and temperature excess $\Delta T/T_o$ are plotted vs $M = 2M_{co}$; the maxima occur at the layer centerline. For small Mach numbers $M < 1$, $M_t \propto M$, and rms fluctuating speed $q \propto \Delta U$. However, for $M > 3$, M_t approaches an asymptotic limit $M_{t\infty}$, suggesting that turbulent fluctuations are controlled by the local sonic speed, i.e. $q \propto a(T)$.

An important aspect of the model results presented in Figs. 1 and 2 is that their qualitative features are independent of the details of the turbulence closure, or of the exact form of the dissipation function $F(M_t)$, which determines ε_d. Thus, these results and findings can be considered as generally valid and not the property of the model. They form the starting point and basis of a similarity theory for supersonic mixing layers, which is the principal subject of this paper (Sec. III). In Sec. IV we describe the Reynolds stress closure model employed to simulate the mixing layer (hereafter referred to as RSM model), and present model computations to validate the proposed similarity theory. Parameterization of basic properties of the supersonic mixing layers is also proposed. Section V deals with certain aspects of the dynamics of baroclinic and temporarily growing shear layers, and suggests ways to account for the baroclinic, or variable density, effects in the similarity solutions. Summary and conclusions are in Sec. VI. In the following section, the equations governing compressible turbulent shear-layers are presented.

II. Favre-Averaged Equations of Motion

The basic conservation equations for compressible flows are the momentum equation (for ρU_i), the energy equation for static enthalpy $H = c_pT$, the mass conservation equation (for density ρ), and the ideal gas law (see e.g., Liepmann and Roshko).[10] The viscosity μ and thermal conductivity κ are assumed to be functions of mean temperature only; in deriving the turbulence moment equations, fluctuations in μ and κ are neglected. The molecular Prandtl number is assumed to be constant and the bulk viscosity zero. To formulate the mean and turbulence transport equations, we employ Favre averaging. The Favre average of a stochastic variable X is defined as $\tilde{X} = \overline{\rho X}/\bar{\rho}$ where the overbar denotes the Reynolds, or ensemble average. Note that the Reynolds average of the fluctuating parts $u_i = U_i - \tilde{U}_i$ and $h = H - \tilde{H}$ are nonzero and that pressure $P = \bar{p} + p$, and density $\rho = \bar{\rho} + \rho'$ are Reynolds-averaged.

In shear layers of practical interest, the turbulent Reynolds number $R_e = u'\ell/\nu$ is large enough to neglect terms of order $O(R_e^{-1})$ or smaller and the Favre-averaged equations for ρ, U_iH, and P can be written as

$$\frac{\partial\bar{\rho}}{\partial t} + \tilde{U}_j\frac{\partial\bar{\rho}}{\partial x_j} = \frac{D\bar{\rho}}{Dt} = -\bar{\rho}\nabla\tilde{U}_{j,j} \tag{1}$$

$$\bar{\rho}\frac{D\tilde{U}_i}{Dt} = -\frac{\partial\bar{p}}{\partial x_i} - \frac{\partial\bar{\rho}\widetilde{u_iu_j}}{\partial x_j} \tag{2}$$

$$\bar{\rho}\frac{D\tilde{H}}{Dt} = \frac{D\bar{p}}{Dt} - \frac{\partial\bar{\rho}\widetilde{hu_j}}{\partial x_j} + \frac{\partial\overline{pu_j}}{\partial x_j} + \bar{\rho}\varepsilon_{tot} - \overline{pu_{j,j}} \tag{3}$$

$$\bar{p} = \bar{\rho}R\tilde{T} = \bar{\rho}R\tilde{H}c_p^{-1} \tag{4}$$

Closure of the above equations requires knowledge of the Favre-averaged Reynolds stresses $\widetilde{u_iu_j}$, enthalpy fluxes $\widetilde{hu_j}$, total energy dissipation ε_{tot}, and the pressure containing terms $\overline{pu_j}$, and $\overline{pu_{j,j}}$. The transport equations for $\widetilde{u_iu_j}$ and $\widetilde{hu_j}$ are given, for example, in Dussauge and Gaviglio.[11] Equations (1–4) can be simplified by invoking the thin-layer approximation whereby the terms of order $\ell/x \propto d\delta/dx$ are neglected (Tennekes and Lumley).[12] The pivotal assumption that $d\delta/dx << 1$ is well satisfied in compressible shear layers and Eqs. (1–4) reduce to

$$\frac{\partial\bar{\rho}\tilde{U}_j}{\partial x_j} = 0 \tag{5}$$

$$\bar{\rho}\tilde{U}_j\frac{\partial\tilde{U}_1}{\partial x_j} = \frac{\partial\bar{\rho}\widetilde{u_1u_2}}{\partial x_2} \tag{6}$$

$$c_p\bar{\rho}\tilde{U}_j\frac{\partial\tilde{T}}{\partial x_j} = -\frac{\partial\bar{\rho}\widetilde{hu_2}}{\partial x_2} + \frac{\partial\overline{pu_2}}{\partial x_2} + \rho\varepsilon_{tot} - \overline{pu_{j,j}} \tag{7}$$

$$\bar{p} = \frac{p_o}{R\tilde{T} + \widetilde{u_2^2}} \tag{8}$$

Equation (8) contains the thin-layer assumption that the mean static pressure $\bar{p}$ within the turbulent region satisfies the constraint $\bar{p} + \bar{\rho}\widetilde{u_2^2} = p_o$ where p_o is the static pressure in the freestreams. From the fluctuating pressure equation $p = (\rho h + \rho'\tilde{H})R/c_p$, inferred from the gas state law, it is readily shown that

$$\overline{pu_i} = (\bar{\rho}\widetilde{hu_i} + \overline{\rho'u_i}H)\frac{R}{c_p} \tag{9}$$

In the incompressible limit, $\overline{pu_i}$ tends to zero; for finite M_t, we expect a dependence $\overline{pu_i} = (R/c_p)(\bar{\rho}\widetilde{hu_i})f_p(M_t)$ with the asymptotic behavior $f_p \to M_t^2$ as $M_t \to 0$, and $f_p(M_t) \to$ const, when M_t approaches the saturation limit $M_{t\infty}$ (for $M > 3$). Hence, the pressure flux $\overline{pu_2}$ in Eq. (7) can be combined with

the enthalpy flux term so that the total energy flux is

$$\overline{\rho h u_2} - \bar{\rho}\bar{u}_2 = \bar{\rho}\widetilde{hu}_2\left(1 - f_p(M_t)\frac{R}{c_p}\right) \tag{10a}$$

The total dissipation ε_{tot} is a heat source in the energy Eq. (7). It consists of solenoidal and dilatation contributions and can be expressed as

$$\varepsilon_{tot} = \varepsilon_s + \varepsilon_d = \varepsilon_s[1 + F(M_t)] \tag{10b}$$

The solenoidal dissipation ε_s is considered here as independent of the compressibility effects and is known to scale on u'^3/ℓ. In κ-ε, or second-order closure models it is determinable from a standard model equation. In Ref. 6, the dilatation dissipation function F was determined from an integral expression which involves a probability distribution function of fluctuating Mach number $(u_i^2/a^2)^{1/2}$. For mixing layer computations in Ref. 6, F was approximated by:

$$F(x) = 0.75[1 - \exp\{-[(x - 0.1)/0.6]^2\}]$$

$$F(x) = 0 \text{ if } x \le 0.1 \tag{10c}$$

In general, the function F depends strongly on the intermittency of the turbulence field and it may be different in different types of flow. The important parameter determining F is the kurtosis of the Mach number fluctuations.

For the purpose of similarity analysis, it is more convenient to deal with turbulence energy production rather then with dissipation. In the turbulence energy budget of mixing layers about 90% of the turbulence (shear) production is dissipated, and the remaining 10% accounts for the layer growth. Furthermore, as found by Zeman and Blaisdell[13] (also Ref. 8 and Zeman[14]), the pressure-dilatation $\overline{pu_{j,j}}$ in homogenous shear turbulence is a small (asymptotically constant) fraction of $\bar{\rho}\varepsilon_s$. Hence, the last two terms in Eq. (7) can be combined and made proportional to the turbulence production, so that

$$\bar{\rho}\varepsilon_{tot} - \overline{pu_{j,j}} \approx -0.9\bar{\rho}\widetilde{u_1 u_2}\frac{\partial U_1}{\partial x_2} \tag{11}$$

III. Similarity Analysis

Now, Eqs. (5–8) with the closures in Eqs. (10a) and (11) are in a suitable form for the similarity analysis. For the sake of simplicity, we deal with isothermal freestreams with $T_1 = T_2 = T_o$, and proceed in a manner analogous to that in Ref. 12 for low-speed free-shear layers; alternative coordinate systems $(x, y, z) = (x_1, x_2, x_3)$ are used throughout the text. The principal objective of the following analysis is to establish that there exist solutions for $U_1 = U(x, y)$, and $T(x, y)$, of the form

$$U = U_c + \Delta U f(\eta) \tag{12}$$

$$T = T_o + \Delta T\theta(\eta) \tag{13}$$

Here $\eta = (y - y_c)/\delta_\omega$ is the similarity variable for the transverse distance with the origin at the shear layer centerline y_c. The scaling length δ_ω is the vorticity thickness defined as $\delta_\omega = \Delta U/(\partial U/\partial y)_c$, and $\Delta T = T_c - T_o$ is the temperature excess. The appropriate boundary values are $f = 0$, $\theta = 1$ at $\eta = 0$, and $f = \pm 1/2$, $\theta = 0$ at $\eta = \pm\infty$. Now, the similarity functions $f(\eta)$ and $\theta(\eta)$ can exist only if their differential equations are independent of the parameters of the flow. In the isothermal shear layer, the independent parameters are the Mach number $M = \Delta U/a_o = 2M_{co}$, and the ratio $\Delta U/U_{co}$. Because $\rho_1/\rho_2 = 1$, the convective velocity is $U_{co} = (U_1 + U_2)/2$, coinciding with the centerline velocity U_c.

In compressible shear layers we assume that the concept of eddy viscosity (and diffusivity) remains valid and that the turbulent Prandtl number $P_{rt} = K/K_h = O(1)$ is constant. Furthermore, by the scaling analysis of Eq. (7), it can be shown that

$$\Delta T/T_o = \alpha M^2 \tag{14}$$

The proportionality constant α has been estimated from the RSC model simulations[6] shown in Fig. 2 as $\alpha = 0.05$. Finally, by substituting expressions in Eqs. (12) and (13) into Eqs. (6) and (7), we obtain ordinary differential equations

$$-\frac{\delta'_\omega U_c}{\Delta U} f' \int_0^\eta \bar{\rho}\left(1 + \frac{\Delta U}{U_c} f\right) d\eta = \frac{K_c}{\Delta U \delta_\omega}\left(\frac{K}{K_c}\bar{\rho} f'\right)' \tag{15}$$

$$-\frac{\delta'_\omega U_c}{\Delta U}\theta' \int_0^\eta \bar{\rho}\left(1 + \frac{\Delta U}{U_c} f\right) d\eta$$

$$= \frac{K_c}{\Delta U \delta_\omega}[(\gamma P_{rt})^{-1}\left(\frac{K}{K_c}\bar{\rho}\theta'\right)' + \beta\bar{\rho}\frac{K}{K_c}(f')^2] \tag{16}$$

Here, primes denote derivatives with respect to η, and K_c is the centerline (maximum) eddy viscosity that is expected to be a function of M. The presence of the specific heat ratio γ in Eq. (16) results from setting the maximum of the pressure-flux function $f_p(M_t)$ in Eq. (10a) to unity. This approximation is justified when the centerline M_t reaches the asymptotic (saturation) value $M_{t\infty}$. The last term in Eq. (16) represents the (normalized) dissipation heat source ε_{tot}/c_p. According to Eq. (11) this term is proportional to the turbulence production rate and the associated constant β in Eq. (16) is related to the constant α by $\beta = 0.9\alpha^{-1}R/c_p \approx 5.0$. The heat source term is responsible for the density variation and coupling of the momentum and energy Eqs. (15) and (16). In view of the similarity analysis, it is important to note that:

1) According to experimental evidence[1,2,3,4,5] and the model results,[6] the layer growth rate parameter $\delta'_\omega U_c/\Delta U$ appearing in Eqs. (15) and (16) is a function of M.

2) The turbulent Reynolds number $R_T = \Delta U\delta_\omega/K_c$ is also a function of M, because by definition

$$R_T^{-1} = \frac{K_c}{\Delta U\delta_\omega} = \frac{u_*^2}{\Delta U^2} \tag{17}$$

The ratio $u_*/\Delta U$ has been observed to decrease with M (e.g., Ref. 5).

3) Equations (15) and (16) also contain the independent parameter $\Delta U/U_c$; without loss of generality, we shall assume in the following considerations that $\Delta U/U_c << 1$ and that the layer evolves in time.

4) The density $\bar{\rho} = \rho_o(1 + \alpha M^2\theta(\eta))^{-1}$ cannot be expressed as a similarity function, and therefore, in principle, the assumed similarity functions $f(\eta)$, $\theta(\eta)$ do not exist unless $M \to \infty$. However, as we see in the following, the nonsimilar variation of density is not critical to the analysis; the model-computed functions tend to self-similar forms in the layer bulk when M reaches about 3 and we expect this to be the case in the real-world supersonic mixing layers as well.

In the proximity of the layer centerline $\theta(\eta)$ is close to unity and the density can be expanded in a Taylor series:

$$\frac{\bar{\rho}}{\rho_c} = 1 - \frac{1}{(1 + \alpha M^2)^2}\theta''(0)\frac{\eta^2}{2} + O(\eta^3)$$

and, hence, to second order in η, the profile of $\bar{\rho}/\rho_c$ can be considered as a similarity function. This also implies that unless the Mach number M is very large, the similarity may be satisfied only in the core of the shear layer. With these limitations in mind, we can proceed with the analysis of Eqs. (15) and (16).

Requirements for the existence of similarity solutions are that: 1) eddy viscosity profiles K/K_c be functions of η only, independent of M; and 2) the coefficients of the differential Eqs. (15) and (16) be proportional to each other, i.e.:

$$C_\delta = \frac{\delta'_\omega U_c}{\Delta U} \propto \frac{1}{R_T} = \frac{u_*^2}{\Delta U^2} \tag{18}$$

As in low-speed mixing layers, the first requirement is expected to be satisfied. The profiles of K/K_c inferred from the RSC-model simulations are shown in Fig. 3; as M increases, K/K_c converges roughly to a single curve, or the similarity profile. The second requirement embodied in the relations in Eq. (18) is satisfied if we accept the earlier mentioned argument that the maximum rms. Mach number M_t reaches a saturation limit $M_{t\infty}$. The existence of the saturation limit is at present supported only by model results shown in Fig. 2. However, because these results are independent of the model details, they can be considered as generally valid. All Reynolds stress components must then be limited by an upper bound dictated by the local sonic velocity, or

$$\left(\frac{\widetilde{u_i u_j}}{a^2}\right)_c \propto \frac{u_*^2}{a_c^2} \propto \left(\frac{q^2}{a^2}\right)_c = M_{t\infty}^2 \tag{19}$$

where the centerline sonic speed a_c is related to the freestream value a_o by

$$a_c^2 = a_o^2(1 + \Delta T/T_o) = a_o^2(1 + \alpha M^2) \tag{20}$$

Combining Eqs. (18) and (19) we obtain the first principal result of our analysis: that the nondimensional growth rate C_δ is related to the mean Mach number M in the following way:

$$C_\delta \propto \frac{u_*^2}{\Delta U^2} \propto \frac{1 + \alpha M^2}{M^2} \tag{21}$$

Evidently, the second similarity requirement provides a parametric formula for a mixing layer growth when M is sufficiently large. A relation similar to Eq. (21) can be inferred from the integral momentum equation which, in a thin-layer approximation, yields:

$$C_\delta \int_0^\infty \rho(1/2 - f(\eta))d\eta \approx \frac{u_*^2}{\Delta U^2}\rho_c \tag{22}$$

IV. Similarity Solutions from Model Computations

At the present time, in supersonic mixing layers there are virtually no experimental data for sufficiently high convective Mach numbers to verify the proposed similarity theory. The only alternative is utilization of model results. We employed the RSC model[6] whose results have already been presented in Figs. 1–3. The model represents all the important mechanisms expected to be present in supersonic mixing layers. It compares well with the available data on Reynolds stresses[5] in the range of convective Mach numbers 0.5 to 1, and it is expected to be realistic at higher Mach numbers as well.

The numerical scheme and turbulence model equations employed in the RSC model are given in Ref. 6. The scheme utilizes the von Mises transformation, so that integration in streamwise direction x_1 is performed along streamlines ψ = const. This approach eliminates the mean transverse velocity from the equations of motion and greatly simplifies computations. Apart from the added dissipation ε_d, the turbulence model equations for the Favre-averaged turbulent stress components $\widetilde{u_i u_j}$ are the same as their incompressible counterparts (for the Reynolds averaged stresses $\overline{u_i u_j}$). All modeled pressure terms have the same form as in the incompressible case. For model details, the interested reader is referred to Ref. 6, and also to Zeman and Jensen[15] and Ref. 13. The model computations presented in the following were performed for different values of the Mach number M but with a fixed value of the parameter $\Delta U/U_c = 0.2$.

In Fig. 4 normalized growth rates $\delta'_\omega/\delta'_{\omega o}$ of the vorticity thickness are presented. The solid line represents the RSC model results and the dashed line represents the relationship

$$\frac{\delta'_\omega}{\delta'_{\omega o}} = 1.65\,\frac{1 + \alpha M^2}{M^2} \tag{23}$$

which is based on the similarity requirement in Eq. (21). Here $\delta'_{\omega o}$ refers to the growth rate at $M = 0$ and $\alpha = 0.05$ from Eq. (14). The parametric expression in Eq. (23) agrees well with the model simulations above $M = 3$, as expected. Note that for large values of M, the normalized growth rates $\delta'_\omega/\delta'_{\omega o}$ inferred from the model simulations approach a value of about 0.075, which is by a factor of two smaller than the experimental growth rates. This difference is likely due to different definitions of the shear layer thickness; in experiments the thickness is usually inferred from dynamic-pressure, or momentum profiles,[1,2,5] which typically yield larger growth rates than those based on the vorticity thickness δ_ω.

To demonstrate the high Mach number similarity, we present in Figs. 5–8 the profiles of the principal mean and turbulence quantities in the shear layer for increasing value of M. It is seen that these quantities do converge to self-similar forms. The most rapid convergence to similarity is exhibited by the mean velocity function $f(\eta)$ shown in Fig. 5. This is because the constitutive relationship between Favre-averaged

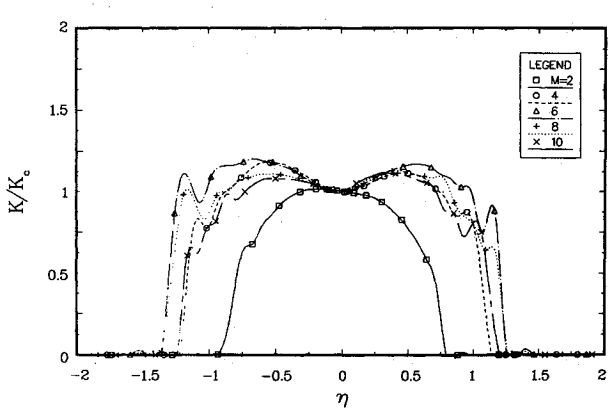

Fig. 3 Model-computed profiles of normalized eddy viscosity for different Mach numbers M.

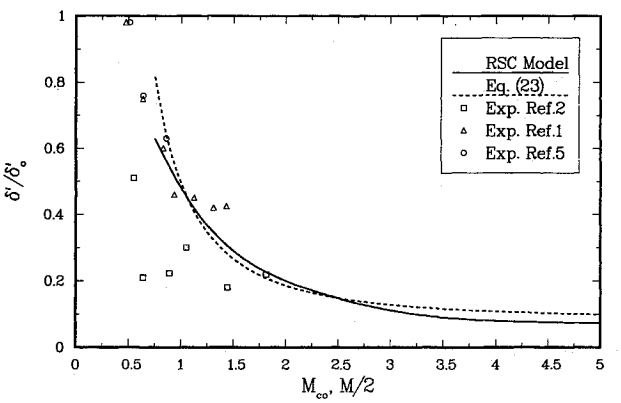

Fig. 4 Comparison of shear-layer growth rates based on vorticity thickness δ_ω. The solid line represents model simulations; the dashed line is based on the parametric expression in Eq. (23); experimental data are same as in Fig. 1 with data points for $M_{co} < 0.5$ deleted.

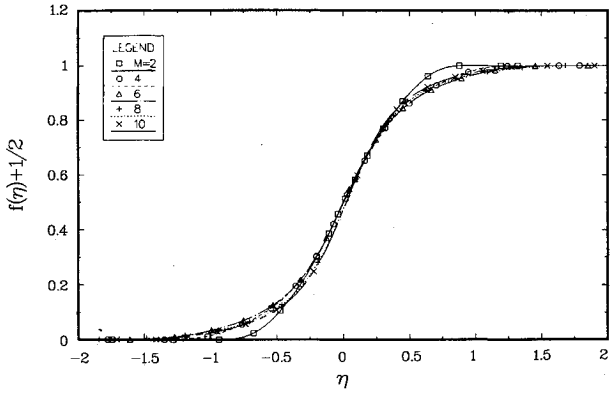

Fig. 5 Model profiles of the velocity similarity function $f(\eta) + 1/2$ computed for different values of M.

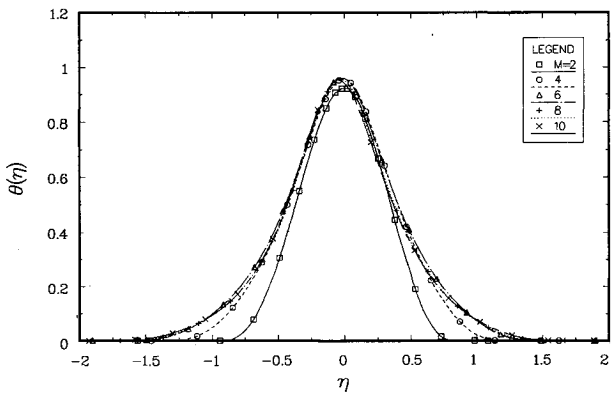

Fig. 6 Model profiles of the temperature similarity function $\theta(\eta)$ computed for different values of M.

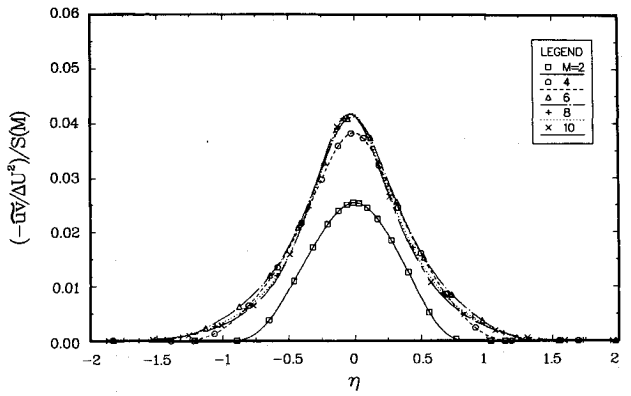

Fig. 7 Model profiles of the normalized Reynolds shear stress computed for different values of M.

shear stress $\widetilde{uv}$ and the mean shear is independent of density variation. The temperature profiles plotted in Fig. 6 indicate a convergence to similarity for $M \geq 4$. It is to be noted that in order to improve the profile convergence, the exponent in the Mach number function for $\Delta T/T_o$ was altered to $\Delta T/T_o = \alpha M^{2.1}$. The same exponent appears in the scaling coefficient $S(M) = (1 + \alpha M^{2.1})M^{-2}$ for Reynolds stress profiles $-\widetilde{uv}/\Delta U^2$, $\widetilde{v^2}/\Delta U^2$ as suggested by the relations in Eqs. (19–21). The noninteger exponent results in better overall convergence of profiles; the noninteger part is relatively small and perhaps accounts for the effects that are excluded from the similarity analysis. The convergence of the Reynolds stress profiles in Figs. 7 and 8 to a single curve is rather remarkable considering the approximate nature of the expression for the scaling factor $S(M)$. We note that the profiles converge much slower at the

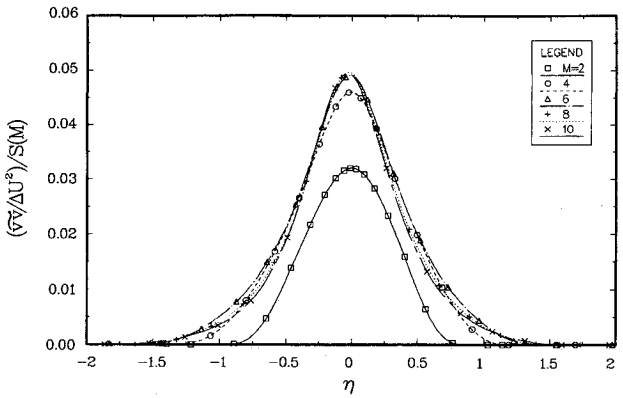

Fig. 8 Model profiles of the normalized transverse velocity variance computed for different values of M.

layer edges. This is likely caused by the nonsimilar nature of the mean density as discussed above. Based on the visual inspection of the profiles in Figs. 5–8 we can conclude that the proposed high Mach number similarity holds well within the bulk of the mixing layer for Mach numbers exceeding $M = 3$.

For the practical purposes, it is convenient to express the results of the preceding analysis in the form of parametric laws for the basis mixing layer quantities. These are as follows:

$$C_\delta = \delta'_\omega U_c/\Delta U = 0.165S(M)$$

$$T = T_o(1 + \alpha M^{2.1}\theta(\eta)), \quad U = U_2 + \Delta U(f(\eta) + 1/2)$$

$$-\widetilde{uv}/\Delta U^2 = 0.0425S(M)g_{12}(\eta)$$

$$v^2/\Delta U^2 = 0.052S(M)g_{22}(\eta)$$

$$u^2/\Delta U^2 = 0.11S(M)g_{11}(\eta) \tag{24}$$

where

$$S(M) = \frac{1 + \alpha M^{2.1}}{M^2}$$

The above expressions were obtained from model computations with $\Delta U/U_c = 0.2$ with isothermal freestream conditions, and they should be applicable for $M \geq 3$. The unspecified similarity functions $\theta(\eta)$, $g_{ij}(\eta)$ are approximately symmetric and Gaussian-shaped, and $f(\eta)$ is close to an error function. However, as the parameter $\Delta U/U_c$ increases beyond 0.4, the similarity profiles become progressively more skewed. Nevertheless, according to computations, the Reynolds stress and temperature levels near centerline retain the values given in the parametric formulae in Eq. (24).

V. Remarks on Baroclinic Effects and Temporal Mixing Layers

Real mixing layers are rarely isothermal, i.e., with equal temperatures and densities in the freestreams. Frequently, in the experiments the freestream density values are dictated by the constant total enthalpy constraint so that the fast stream is denser than the slow one. The mixing layer is then called baroclinic. As suggested in Ref. 2, the baroclinic effect on the layer growth rate can, to a large extent, be accounted for by redefining the convective velocity U_{co}:

$$U_{co} = \frac{U_1 a_2 + U_2 a_1}{a_1 + a_2} \tag{25}$$

Hence, if the fast stream is denser than the slow one, i.e., if

the density ratio $\rho_2/\rho_1 = r < 1$, U_{co} will be larger than the isothermal value $(U_1 + U_2)/2$ and vice versa. It follows that for a given convective Mach number $M_{co} = (U_1 - U_{co})/a_1$ (see Ref. 2), the absolute growth rate $\delta'_\omega \propto \Delta U/U_{co}$ will depend on the density ratio r, because with the assumption of constant pressure $r = (a_2/a_1)^2$. This alteration of the growth rate has a simple physical explanation: if the fast stream is denser $r < 1$, the large eddies traveling at a speed $\propto U_{co}$ reach further downstream than in the isothermal case, and provided that the transverse eddy growth rate and pairing are little affected by baroclinity, the average spatial growth will be lower; the opposite is true if $r > 1$. The RSC model[6] reproduces the baroclinic effect on growth rate. This effect can be traced to the shear-stress gradient term in the mean momentum Eq. (6). In the presence of baroclinity, we can identify at $y = y_c$ an acceleration term:

$$U_1 \frac{\partial U_1}{\partial x_1} \propto -\frac{\partial \ell_n(\rho)}{\partial x_2} \widetilde{uv}_c \propto \frac{(1 - r)u_*^2}{(1 + r)\delta_\omega} \tag{26}$$

Obviously, this term will either accelerate ($r < 1$) or decelerate ($r > 1$) the bulk of the mixed fluid, which is equivalent to increasing or decreasing the convective velocity U_{co}.

Inspection of the equations of motion indicates that similarity analysis of baroclinic compressible mixing layers is too complex to yield useful results. However, it is likely that the parametric expression for layer growth rate proposed in Eq. (24) is valid even in baroclinic mixing layers, provided that the density ratio r is not too extreme. In the parametric expressions (24), M must be replaced by an effective Mach number $2M_{co}$, and U_c by U_{co} determined from Eq. (25).

A temporally growing mixing layer can be considered as a spatially growing layer in the limit $\Delta U/U_c \to 0$. Direct numerical simulations of a two-dimensional compressible shear layer suggest that the normalized temporal growth rate:

$$C_\delta^t = \frac{(\delta_\omega)_t}{\Delta U}$$

varies with M_{co}, as in the spatially growing layer (Lele[16]). However, there is a difference between the spatial and temporal growths in the baroclinic case. The temporal layer growth must be independent of the density ratio r, because in the temporal layer one cannot distinguish between fast and slow streams. Another way to view the temporal growth is to note that because the temporal layer is the limit $\Delta U/U_c \to 0$ of the spatial layer, the convective velocity U_{co} loses its physical significance and therefore the growth rate must be independent of r. The only way the unequal densities affect the temporal growth, is a layer drift away from its initial transverse location toward the stream with lower density. The cause of the drift can be traced again to the baroclinic term in Eq. (26). An interesting aspect of the compressible mixing layer is the existence of the finite transverse velocity $\tilde{U}_2 \equiv \tilde{V}$ away from the layer, which is absent in the low-speed case. By scaling analysis, it can be shown that for $r = 1$, $\tilde{U}_2$ scales on

$$V_o = (\gamma - 1)M^2 u_*^2/\Delta U \tag{27}$$

Hence, for sufficiently large M, the x_2-advection term in the convective derivative can be of the same order as the temporal term. We note that in the limit $M \to 0$, $u_*/\Delta U$ approaches a constant, so that V_o tends to zero as $V_o \to M^2 u_*$.

To demonstrate the aforementioned peculiarities of the temporal layer, calculations were made with the same RSC model as discussed before (Ref. 6) with a temporal integration scheme. Because the mean transverse velocity $\tilde{U}_2$ is nonzero, the convective derivative in the temporal conservation equations is $D/Dt \equiv \partial/\partial t + \tilde{U}_2 \partial/\partial x_2$, and the transverse velocity $\tilde{U}_2$ is obtained from the Favre-averaged mass conservation equation

$$\frac{\partial \bar{\rho}}{\partial t} + \frac{\partial(\bar{\rho}\tilde{U}_2)}{\partial x_2} = 0$$

The temporal model results are presented in Figs. 9 and 10. The time sequence of the model-computed mean velocity profiles for two cases with $r = 3$, and 1/3 in Fig. 9 demonstrate the layer drift. While the layer spreading rate remains the same for both cases, the drift toward the low density side is evident. The evolution of model-computed profiles of the normalized transverse velocity $\tilde{U}_2/V_o$ at $M = 4.0$ is shown in Fig. 10. It is seen that the modeled flow approaches a self-preserving state within a time $t = 2$s. which, in terms of the mixing layer time-scale, represents $t\Delta U/\delta_o = 1000$. The outward velocity outside the layer is then about $0.71V_o$.

VI. Conclusions

In the paper, similarity in supersonic mixing layer has been explored. On the basis of theoretical considerations and model simulations, it has been found that a self-similar state is reached when the shear layer Mach numbers M exceeds a value of about 3. The similarity rests mainly on the assumption that or $M \geq 3$, the rms Mach number reaches a saturation limit $M_{t\infty} \approx 0.5$.

On the basis of the similarity and model results, a parameterization of the supersonic mixing layers has been explored. The parametric expressions Eq. (24) furnish first order estimates of the properties of supersonic shear layers. For given freestream velocities and temperatures, these expres-

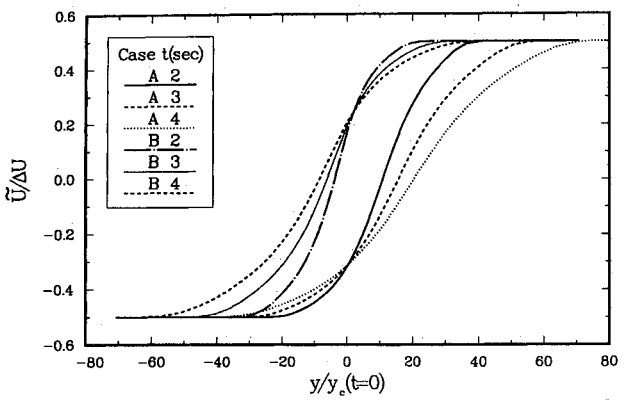

Fig. 9 Model-simulated evolution of mean velocity profiles for two different baroclinic temporal shear layers at $M = 4$. Case A: $r = \rho_2/\rho_1 = 3$; Case B: $r = 1/3$. The evolution times $t = 2$, 3, and 4 s represent $t\Delta U/\delta_o = 1000$, 1500, and 2000.

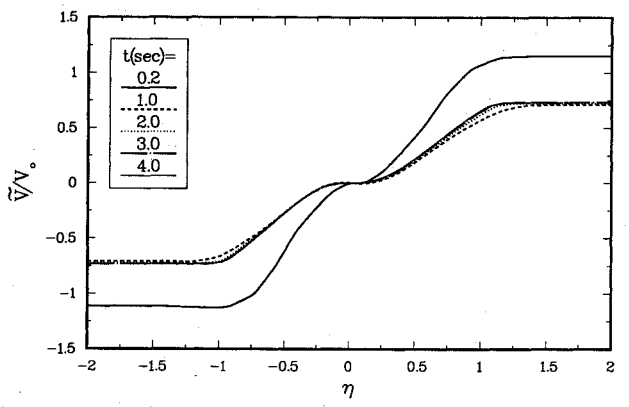

Fig. 10 Evolution of the model-simulated profiles of mean transverse velocity in a temporal shear layer with $M = 4$. The normalizing velocity V_o is defined in Eq. (27).

sions provide estimates of the layer growth rate, temperature excess, and Reynolds stresses.

Moderate baroclinic effects due to unequal densities in the freestreams of the mixing layer are accounted for in the RSC model[6] through the baroclinic acceleration term in the mean momentum equation. This term influences the bulk velocity of the mixing layer fluid, thus, changing the convective velocity of the large-scale eddies.

Finally, it has been shown that in temporally growing shear layers, the growth rate is affected by baroclinity. The principal effect of the unequal stream densities is the shear layer drift toward the stream with lower density.

Acknowledgments

The author thanks Joel Ferziger and Sanjiva Lele for helpful suggestions and revision of this manuscript.

References

[1]Bogdanoff, D. W., "Compressibility Effects in Turbulent Shear Layers," *AIAA Journal*, Vol. 21, No. 6, 1983, pp. 926, 927.

[2]Papamoschou, D., and Roshko, A., "The Compressible Turbulent Shear Layer: An Experimental Study," *Journal of Fluid Mechanics*, Vol. 197, 1988, pp. 453–457.

[3]Ikawa, H., and Kubota, T., "Investigation of Supersonic Turbulent Mixing Layer with Zero Pressure Gradient," *AIAA Journal*, Vol. 13, No. 5, 1975, pp. 566–572.

[4]Chinzei, N., Masuya, G., Komuro, T., Murakami, A., and Kudou, K., *Physics of Fluids*, Vol. 29, No. 5, 1986, p. 134.

[5]Samimy, M., and Elliott, G. S. "The Effects of Compressibility on the Characteristics of Free Shear Layers," *AIAA Journal*, Vol. 28, No. 3, 1990, p. 439.

[6]Zeman, O., "Dilatation Dissipation: The Concept and Application in Modeling Compressible Mixing Layers," *Physics of Fluids A: Fluid Dynamics*, Vol. A2, Feb. 1990, pp. 178–188.

[7]Lee, S., Lele, S. K., and Moin, P., "Eddy Shocklets in Decaying Compressible Turbulence," *Physics of Fluids A: Fluid Dynamics*, Vol. 3, April 1991, pp. 657–664.

[8]Blaisdell, G. A., Mansour, N. N., and Reynolds, W. C., "Numerical Simulations of Compressible Turbulence," Dept. of Mechanical Engineering, Stanford Univ., Rept. TF-50, Stanford, CA, 1991.

[9]Sarkar, S., Erlebacher, G., Hussaini, M. Y., and Kreiss, H. O., "The Analysis and Modeling of Dilatational Terms in Compressible Turbulence," Inst. for Computer Application in Science and Engineering, Rept. 89-79, 1989.

[10]Liepmann, H., and Roshko, A., *Elements of Gas Dynamics*, Wiley, New York, 1967, pp. 319–352.

[11]Dussauge, J. P., and Gaviglio, J., "The Rapid Expansion of a Supersonic Turbulent Flow: Role of Bulk Dilatation," *Journal of Fluid Mechanics*, Vol. 174, 1987, pp. 81–112.

[12]Tennekes, H., and Lumley, J. L., *A First Course in Turbulence*, MIT Press, Cambridge, MA, 1972, p. 300.

[13]Zeman, O., and Blaisdell, G. A., "New Models and Physics for Compressible Turbulent Flows," *Advances in Turbulence 3*, edited by A. V. Johansson and P. H. Alfredsson, Springer-Verlag, Berlin, 1991, pp. 445–454.

[14]Zeman, O., "On the Decay of Compressible Isotropic Turbulence," *Physics of Fluids A: Fluid Dynamics*, Vol. A2, May 1991, pp. 951–955.

[15]Zeman, O., and Jensen, N. O., "Modification of Turbulence Characteristics in Flows over Hills," *Quarterly Journal of the Royal Meteorological Society*, Vol. 113, 1987, pp. 55–80.

[16]Lele, S. K., "Direct Numerical Simulations of Compressible Free Shear Flows," AIAA Paper 89-0374, Reno, NV, 1989.